ISBN: 978-3-95450-231-8 ISSN: 2673-5490 doi: 10.18429/JACoW-IPAC2023-MOPA045

SIMULATION TEST OF VARIOUS CRAB DISPERSION CLOSURE BUMPS FOR THE HADRON STORAGE RING OF THE ELECTRON-ION COLLIDER*

Y. Luo†, J. S. Berg, M. Blaskiewicz, A. Drees, X. Gu, H. Lovelace III,
C. Montag, D. Marx, S. Peggs, V. Ptitsyn, F. Willeke, H. Witte, Q. Wu,
B. Xiao, D. Xu, Brookhaven National Laboratory, Upton, NY, USA
Y. Hao, Facility for Rare Isotope Beams, Michigan State University, East Lansing, MI, USA
H. Huang, B. R. Gamage, T. Satogata,
Thomas Jefferson National Accelerator Facility, Newport News, VA, USA
V. Morozov, Oak Ridge National Laboratory, Oak Ridge, TN, USA

Abstract

The Electron-Ion Collider (EIC) presently under construction at Brookhaven National Laboratory will collide polarized high energy electron beams with hadron beams with luminosities up to $1.0 \times 10^{34}\text{cm}^{-2}\text{s}^{-1}$ in the center mass energy range of 20-140 GeV. To compensate the geometric luminosity loss due to a large crossing angle 25 mrad in the EIC, crab cavities are to be installed on both sides of the interaction point (IP) in both rings to construct a local closed crabbing bump. However, for the current design lattice of the Hadron Storage Ring, the crab dispersion bump is not closed because the ideal 180 degree horizontal phase advance between the crab cavities on both sides of IP cannot be achieved. We carried out numerical simulations to evaluate the impacts of the unclosed crab dispersion bump. We also simulated various closed crab dispersion bumps constructed with artificial phase trombones. We did not observe a significant difference in dynamic aperture between the unclosed and artificially closed crab dispersion bumps. Instead, we observed that the IR magnetic field errors play an more important role to the dynamic aperture than the crab dispersion bump closure.

INTRODUCTION

The Electron-Ion Collider (EIC) presently under construction at Brookhaven National Laboratory will collide polarized high energy electron beams with hadron beams with luminosities up to $1 \times 10^{34}\text{cm}^{-2}\text{s}^{-1}$ in the center mass energy range of 20-140 GeV [1, 2]. Crab cavities will be installed on both sides of the IP in each ring to create a local closed horizontal crab dispersion bump to restore head-on collision condition at the IP.

For the current version of the EIC HSR lattice, the horizontal phase advance between IP6 and the crab cavities is not the ideal 90 degrees. The phase advances between the IP6 and the crab cavities are 87 degrees on the upstream side and 88 degrees on the downstream side of the interaction region (IR). The total phase advance between two side crab cavities is therefore 175 degrees, 5 degrees short of 180 degrees to close the crab dispersion bump locally. Therefore, there is crab dispersion leaking out of the IR and into the rest of ring. The crab dispersion or $\partial x/\partial z$ will introduce an additional horizontal offset depending on the particle's longitudinal position w.r.t. the bunch center. The particles with non-zero z will therefore feel more nonlinear magnetic fields in the IR magnets and also in the arc sextupoles, which may reduce the proton's dynamic aperture [3].

In the following, we will evaluate the impacts on dynamic aperture [4] of the unclosed crab dispersion in the IR6 and also will test various closed bump schemes in the HSR. By inserting artificial phase trombones, we constructed an artificial local 3-bump and 4-bump of horizontal crab dispersion in the IR6, and artificial 3-bump closed between IR6 and IR8. The purpose of this study is to determine the negative impacts from the unclosed crab dispersion bump to the dynamic aperture and the benefits of various artificial closed crab dispersion bumps.

In this study, we adopt an earlier reference lattice with one collision per turn in the IR6. We focus on the collision mode involving 10 GeV electrons and 275 GeV protons. At this collision mode, both electron and proton beams reach their maximum beam-beam parameters in the EIC and its peak luminosity reaches the maximum design peak luminosity $1 \times 10^{34}\text{cm}^{-2}\text{s}^{-1}$. Table 1 list beam-beam related beam and optics parameters used for this study.

Table 1: Beam-beam Related Beam and Optics Parameters for Collision Between 10 GeV Electrons and 275 GeV Protons

quantity	unit	proton	electron
Beam energy	GeV	275	10
Bunch intensity	10^{11}	0.668	1.72
(β_x^*, β_y^*) at IP	cm	(80, 7.2)	(55, 5.6)
RMS Beam sizes at IP	μm	(95, 8.5)	
Bunch length	cm	6	0.7
Energy spread	10^{-4}	6.8	5.8
Transverse tunes		(0.228, 0.210)	(0.08, 0.06)
Longitudinal tune		0.01	0.069

* Work supported by Brookhaven Science Associates, LLC under Contract No. DE-SC0012704 with the U.S. Department of Energy.
† yluo@bnl.gov

ISBN: 978-3-95450-231-8 ISSN: 2673-5490 doi: 10.18429/JACoW-IPAC2023-MOPA045

LEAKAGE OF CRAB DISPERSION

The HSR will have four 197 MHz and two 394 MHz crab cavities on each side of IP6 and they will tilt the proton bunch in the $x - z$ plane by 12.5 mrad to restore head-on collisions at the IP. Ideally, we need 90 degree horizontal phase advance between IP6 and the crab cavities on either side. The minimum requirement is to have 180 degree phase advance between the two side crab cavities to close the crab dispersion bump locally.

Unfortunately, for the current HSR lattice design, the horizontal phase advance between both side crab cavities is 175 degrees from lattice matching. Figure 1 shows the crab dispersion in the ring. With two knobs of total crab cavity voltages on both sides in IR6, we are able to re-match $\partial x/\partial z = 12.5$ mrad and $\partial x'/\partial z = 0$ at IP6. From the plot, the maximum crab dispersion amplitude reaches 35mrad in the IR6, and the maximum crab dispersion amplitude in the arcs reaches 5 mrad.

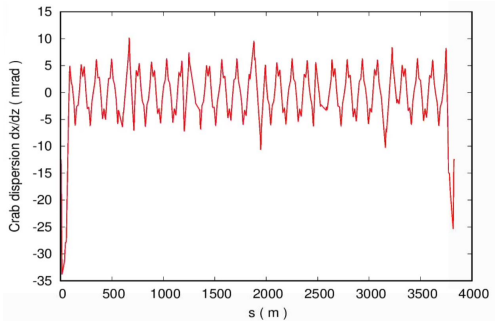

Figure 1: Horizontal crab dispersion in the HSR ring with the unclosed bump in the IR6.

CRAB DISPERSION BUMP SETUP

To assess the impacts of the unclosed crab dispersion bump in the IR6 in the HSR, we also constructed a few closed bumps for comparison. Artificial phase trombones are used to introduce an artificial phase advance at one point in the ring without changing the local Twiss parameters. We need at least two phase trombones to maintain the overall lattice tunes.

First, we insert a phase trombone between the two sets of crab cavities in the IR6 to make the phase advance between them 180 degrees to build a local closed π-bump. We also build a local 3-bump and a local 4-bump in the IR6. For the 3-bump and 4-bump schemes, we added additional crab cavities outside the existing crab cavities.

For the EIC, there are onging studies for a futrure second interaction region at IP8. Therefore, one option is to build a closed 3-bump of crab dispersion between IR6 and IR8. We will install a third crab cavity in IR8. We also simulate a longer 3-bump between IR6 and IR10 for comparison with the 3-bump closed between IR6 and IR8.

Figure 2 shows crab dispersion in the ring with above mentioned crab dispersion bumps. Note that those artifically closed crab dispersion bumps are only for simulation study purpose.

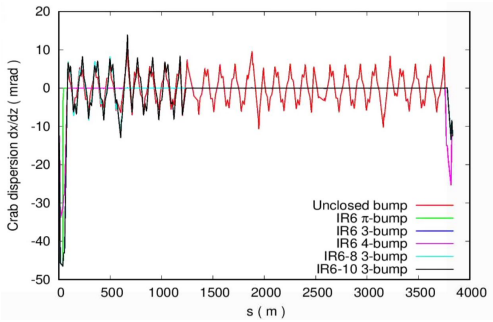

Figure 2: Crab dispersion in the HSR ring for various artificial closed crab dispersion bumps.

DYNAMIC APERTURE CALCULATION

To evaluate the impacts of the unclosed and artificially closed crab dispersion bumps, we calculate the proton's dynamic aperture with the code SimTrack [5]. Test particles are launched in the first quadrant of phase space (x/σ_x, y/σ_y) in 5 equidistant phase angles and tracked up to 1 million turns. We search the minimum dynamic aperture in each direction of those phase angles with a step size of 0.1 σ. In the dynamic aperture calculation, we included random nonlinear magnetic field errors for the IR magnets in the IR6. For each simulation condition, we used 40 seeds of IR nonlinear magnetic field errors.

Head-on vs Crossing Collisions

Figure 3 compares the dynamic apertures with head-on collision and crossing angle collision with the unclosed crab dispersion bump. Both the minimum and the average dynamic aperture of the 40 seeds of IR field errors are shown. From the plot, the average dynamic aperture drops about 3 σ from head-on to crossing angle collisions.

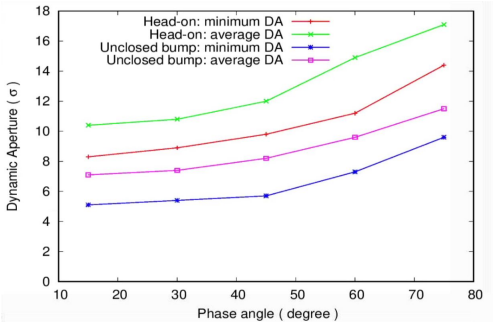

Figure 3: Dynamic aperture with head-on collision and crossing collision with the unclosed crab dispersion bump.

Figure 4 shows the dynamic apertures as function of half crossing angle with the unclosed crab dispersion bump. For each half crossing angle, we re-matched the voltages of crab cavities to restore head-on collision at IP6. From the plot, a larger crossing angle results in a smaller dynamic aperture.

ISBN: 978-3-95450-231-8 ISSN: 2673-5490 doi: 10.18429/JACoW-IPAC2023-MOPA045

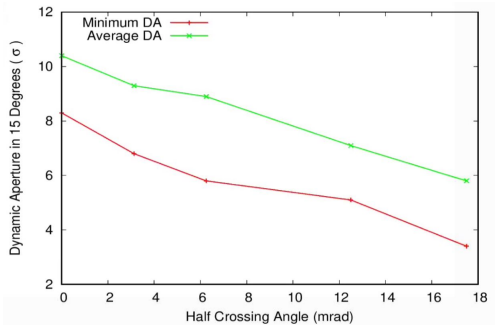

Figure 4: Dynamic aperture as function of crossing angle.

Table 2: Dynamic Aperture for Various Crab Dispersion Closure Bumps

Case Name	Minimum DA	Maximum DA	Average DA	RMS in DAs
head-on	8.3	13.0	10.5	1.0
unclosed	5.1	10.5	7.1	1.6
π bump in IR6	4.6	11.1	7.8	1.5
3-bump in IR6	5.7	10.3	7.6	1.4
4-bump in IR6	4.9	10.7	7.3	1.3
3-bump IR6-8	5.6	10.6	7.6	1.7
3-bump IR6-10	5.0	9.6	6.9	1.3

The dynamic aperture drop with crossing angle collision is caused by the crab dispersion in the IR and the IR nonlinear magnetic field errors. Figure 5 shows the minimum and average dynamic apertures as function of the units of IR field errors with the unclosed crab disperison bump. Clearly, larger IR field errors will result in a lower dynamic aperture.

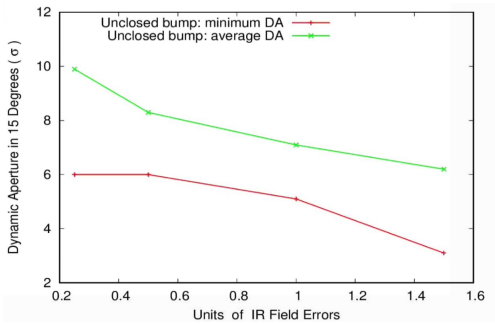

Figure 5: Dynamic aperture as function of IR field errors.

Unclosed vs Closed bumps

Table 2 lists the dynamic aperture calculation results for the unclosed and closed crab dispersion bumps. There is a very small difference between the unclosed and closed bumps. The average dynamic aperture among 40 seeds are all above or very close to 7 σ. However, the minimum dynamic aperture of some cases may drop to 5 σ. According to the RHIC operation experience, the proton dynamic aperture should be larger than 5 σ to provide a sufficient beam lifetime.

Histogram of IR Seeds

Figure 6 shows the histogram of the calculated dynamic apertures for the 40 seeds of IR field errors. From the plot, π-bump and 4-bump in IR6 have more seeds with higher dynamic apertures than the unclosed crab dispersion bump. The way to construct a closed bump, or the phase advances between crab cavities will affect the dynamic aperture too.

Figure 7 shows the dynamic aperture as function of seeds of random IR magnetic field errors. Some seeds always have larger dynamic apertures than other seeds, no matter with what kinds of crab dispersion bumps. This means that the IR magnetic field errors play a more important role to the dynamic aperture than the crab disperison bump closure.

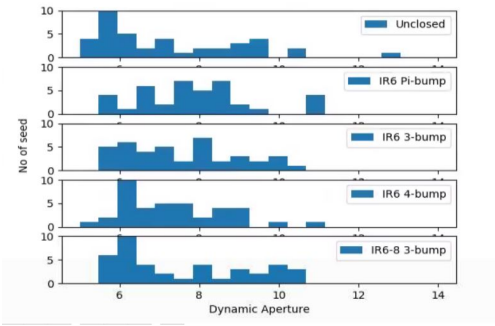

Figure 6: Histogram of dynamic aperture with unclosed and closed crab dispersion bumps.

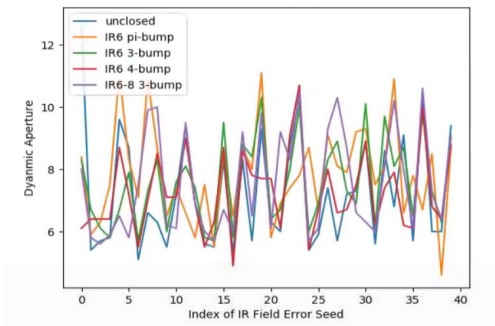

Figure 7: Dynamic aperture as function of seeds of random IR magnetic field errors.

SUMMARY

In this article, we evaluated the impacts of the unclosed crab dispersion bump in the IR6 in the HSR of the EIC. For comparison, we created a few closed crab dispersion bumps with artificial phase trombones. We did not observe a significant difference in dynamic aperture between the unclosed and artificially closed crab dispersion bumps. Instead, we observed that the IR magnetic field errors play an more important role to the dynamic aperture than the crab dispersion bump closure. We will re-visit this topic with a better knowledge of IR magnetic field errors.

ISBN: 978-3-95450-231-8 ISSN: 2673-5490 doi: 10.18429/JACoW-IPAC2023-MOPA045

REFERENCES

[1] J. Beebe-Wang *et al.*, "Electron-Ion Collider: Conceptual Design Report", Brookhaven National Laboratory, Jefferson Lab, 2021. www.bnl.gov/EC/files/EIC_CDR_Final.pdf

[2] C. Montag *et al.*, "Design Status Update of the Electron-Ion Collider", presented at IPAC'23, Venice, Italy, May 2023, paper MOPA049, this conference

[3] Y. Luo *et al.*, "Tolerances of Crab Dispersion at the Interaction Point in the Hadron Storage Ring of the Electron-Ion Collider", in *Proc. NAPAC'22*, Albuquerque, New Mexico, USA, Aug. 2022, paper MOYD5, pp. 12.

[4] Y. Luo, W. Fischer, N. Abreu, X. Gu, A. Pikin, and G. Robert-Demolaize, "Six-dimensional weak-strong simulation of head-on beam-beam compensation in the relativistic heavy ion collider", Phys. Rev. ST Accel. Beams 15, 051004 (2012). doi:10.1103/PhysRevSTAB.15.051004

[5] Y. Luo, "SimTrack: A compact c++ code for particle orbit and spin tracking in accelerators", *Nucl. Instrum. Methods Phys. Res., Sect. A*, vol. 801, pp. 95-103, 2015. doi:10.1016/j.nima.2015.08.014